When Eastern India Oscillated Between Desert Versus Savannah-Dominated Vegetation

Coralie Zorzi, Stéphanie Desprat, Charlotte Clément, Kaustubh Thirumalai, Dulce Oliviera, Krishnamurthy Anupama, Srinivasan Prasad, Philippe Martinez

Geophysical Research Letters

RESEARCH LETTER
10.1029/2022GL099417

When Eastern India Oscillated Between Desert Versus Savannah-Dominated Vegetation

Coralie Zorzi[1], Stéphanie Desprat[1], Charlotte Clément[1], Kaustubh Thirumalai[2], Dulce Oliviera[3,4], Krishnamurthy Anupama[5], Srinivasan Prasad[5], and Philippe Martinez[1]

[1]Environnements et Paléoenvironnements Océaniques et Continentaux (EPOC UMR 5805), Université de Bordeaux, CNRS, EPHE, Université PSL, Pessac, France, [2]Department of Geosciences, University of Arizona, Tucson, AZ, USA, [3]Centro de Ciências do Mar- CCMAR, University of Algarve, Faro, Portugal, [4]Instituto Português do Mar e da Atmosfera - IPMA, Lisbon, Portugal, [5]Laboratory of Palynology & Paleoecology, French Institute of Pondicherry, Pondicherry, India

Key Points:

- Savannah expansion records the highest glacial rainfall in response to an obliquity maximum strengthening of the interhemispheric gradient
- During the last glacial maximum, an open savannah shows low humidy related to large-scale atmospheric reorganization
- Severe droughts occurred in India during the Heinrich Stadials and in response to the Toba eruption, likely amplified by precession

Supporting Information:

Supporting Information may be found in the online version of this article.

Correspondence to:

C. Zorzi,
coralie.zorzi@u-bordeaux.fr

Citation:

Zorzi, C., Desprat, S., Clément, C., Thirumalai, K., Oliviera, D., Anupama, K., et al. (2022). When eastern India oscillated between desert versus savannah-dominated vegetation. *Geophysical Research Letters*, *49*, e2022GL099417. https://doi.org/10.1029/2022GL099417

Received 9 MAY 2022
Accepted 21 JUL 2022

Author Contributions:

Conceptualization: Coralie Zorzi, Stéphanie Desprat, Philippe Martinez
Formal analysis: Coralie Zorzi, Charlotte Clément, Kaustubh Thirumalai
Funding acquisition: Coralie Zorzi, Philippe Martinez
Investigation: Coralie Zorzi
Methodology: Coralie Zorzi, Stéphanie Desprat, Charlotte Clément, Dulce Oliviera, Krishnamurthy Anupama, Srinivasan Prasad
Software: Coralie Zorzi

Abstract During the last glacial period, the tropical hydrological cycle exhibited large variability across orbital and millennial timescales. However, the response of the Indian summer monsoon (ISM), its related impact on terrestrial ecosystems, and associated forcing mechanisms remain controversial. Here we present a marine record of pollen-inferred vegetation changes suggesting that eastern India shifted from woody-savanna mosaics during Marine Isotopic Stage 3 to grasslands during the Last Glacial Maximum resulting from large-scale drying. Our data shows that ISM maximum is in phase with obliquity and precession maxima suggesting a dominant role of the Indian Ocean interhemispheric temperature gradient on glacial ISM variability. Persistent and abrupt dryland expansions of varying magnitude suggest rapid-scale onset of aridity during Heinrich Stadial events and during the Toba eruption. We propose that the amplitude of ISM drought events are initiated by high latitude and volcanic forcings, although modulated by precession.

Plain Language Summary Climatic mechanisms controlling variations in the monsoon rainfalls in India remain unclear even though there is a consensus on the strong vulnerability of this region to the ongoing climate change. Based on the reconstruction of the vegetation in eastern India during the last glacial, our study reveals that very low monsoon rainfall, as indicated by a drastic reduction in trees, occurred when the global ice volume reached its maximum by affecting the global and Indian wind circulations. Conversely, the moistest conditions, as reported by the development of a wooded savannah, are recorded during a period characterized by a specific insolation configuration, which reinforces the temperature contrast over the Indian ocean, and thus the humidity supplied to India. Intense droughts are also documented by the abrupt increases of arid vegetation in response to massive iceberg discharges in the North Atlantic and a major tropical volcanic eruption. We suggest that a low seasonal thermic contrast in the tropical region amplifies the dryness associated with these catastrophic events in India.

1. Introduction

The Indian Summer Monsoon (ISM) appears particularly sensitive to ongoing climate change (Shaw et al., 2022) and its variability could have severe impacts on the future of Indian forest and savannah ecosystems (Ratnam et al., 2016), as well as being a threat to freshwater availability and sustainable agriculture in the near future. Despite predicted ISM intensification (Katzenberger et al., 2021), severe droughts have recently imposed drastic socio-economic conditions across India (Mishra, 2020). In the past, ISM collapses have also led to famines that were unfavorable to the long-term stability of civilizations (Gupta et al., 2006). In order to better understand environmental changes and climatic mechanisms leading to catastrophic weak ISM intervals, our study focuses on the last glacial period over which the tropical hydrological cycle experienced particularly strong and rapid reductions at orbital and millennial time scales.

Previous studies using speleothem records from southern and eastern Asia have argued for a direct ISM response to precession-driven Northern Hemisphere summer insolation changes through its impact on the thermal land-sea contrast (Kathayat et al., 2016; Tharammal et al., 2021). On the other hand, sedimentary records from the Arabian Sea (Clemens & Prell, 2003), the Bay of Bengal (BoB) (Clemens et al., 2021) and northern India (Zhang et al., 2021) point to a predominant role for obliquity in controlling the interhemispheric insolation gradient. Remote forcing factors such as ice-sheet dynamics (Prell & Kutzbach, 1992; Thirumalai et al., 2020), global

Supervision: Stéphanie Desprat, Philippe Martinez
Validation: Coralie Zorzi, Stéphanie Desprat, Kaustubh Thirumalai, Dulce Oliviera, Krishnamurthy Anupama, Philippe Martinez
Writing – original draft: Coralie Zorzi

atmospheric and oceanic circulations (Marzin et al., 2013), and greenhouse gas concentrations (GHGc) (Yan et al., 2011) have also been proposed as additional drivers of ISM fluctuations.

Rapid ISM fluctuations have been recorded concurrent to the occurrences of North Atlantic Heinrich Stadial (HS) events, as well as during Greenland Stadial (GS) and Interstadial (GI) events (e.g., Corrick et al., 2020; Kathayat et al., 2016; Lauterbach et al., 2020). But, the associated changes in terrestrial ecosystems due to changes in ISM rainfall on millennial timescales in the Core Monsoon Zone (CMZ) of India are poorly constrained. Another ongoing debate lies on the modulation of the tropical hydroclimatic events by astronomical forcing. For instance, the potential role of orbital forcing (precession) in controlling the amplitude of the millennial East Asian summer monsoon (EASM) changes is a matter of ongoing discussion (Cheng et al., 2016; Thirumalai et al., 2020; Zhang et al., 2021). However, the variability of terrestrial vegetation impacts in the Indian monsoon sytem over orbital and millennial timescales as well as due to their interconnections remain largely unexplored.

2. Material and Methods

2.1. Site U1446 Climatology and Vegetation

We investigated samples from the International Ocean Discovery Program (IODP) Site U1446 (19°5′N, 85°4′E, 1,430 m water depth; Figure 1) drilled in the BoB and located at the exit of the Mahanadi, one of the major rivers of eastern India strategically situated in the CMZ (Figure 1). Four main ecological groups characterize the vegetation of the Mahanadi catchment (Blasco et al., 1996, 2000; Champion & Seth, 1968; Figure 1) where 80%–90% of precipitation resulted from summer monsoon precipitation (mainly of June to September) (Bastia & Equeenuddin, 2016): the semi-evergreen forest, the tropical moist deciduous forest, the tropical dry deciduous forest and the mangrove. The dry forest has a developed grassy understorey dominated by C4 grasses and was recently reconsidered as a savannah formation (Ratnam et al., 2011, 2016, 2019; Riedel et al., 2021; Sankaran & Ratnam, 2013). Distribution of the ecological groups directly depends on the total annual rainfalls and their seasonality, excepted for the mangrove restricted in the coastal and mainly affected by edaphic factors (Gaussen et al., 1973). The semi-evergreen forest extends in a small area close to coast collecting the highest regional rainfall reaching locally 2,000 $mm.yr^{-1}$. On the other hand, the tropical moist deciduous forest develops at higher altitudes in association with rainfall of ∼1,300–2,000 $mm.yr^{-1}$, whereas the savannah spreads in low-land areas with less humid conditions and rainfall of ∼900–1,300 $mm.yr^{-1}$.

2.2. Pollen Analysis

Our study is based on the analysis of pollen grains and spores from 138 samples with a total of 109 morphotypes identified in this study and a minimum of 150 pollen grains counted per sample. Palynomorph preservation throughout the studied sequence is excellent as shown by the rare occurrence of broken and corroded grains (Figure S3 in Supporting Information S1). The samples were prepared following the standard procedure used at EPOC laboratory (https://www.epoc.u-bordeaux.fr/index.php?lang=fr%26page=eq_paleo_pollens). After chemical treatments (cold HCl and HF), the samples were sieved through 5 µm nylon mesh screens. The final residue was mounted unstained in glycerol, which allowed the mobility of the pollen grains to optimize their observation. The pollen grains were identified and counted using a LEICA DM750 light microscope at 400X and 1000X (oil immersion) magnifications. Marine sediments from the eastern Indian margin, close to the Mahanadi River estuary, have shown that their marine pollen assemblages provide an integrated picture of the regional vegetation of the near continent and more specifically of the nearest river watershed (Sánchez-Goñi al., 2018; Zorzi et al., 2015). Moreover, at Site U1446, transfer of particulate terrestrial material, including pollen grains, is particularly active due to the narrowness of the continental shelf ∼25–60 km (Clemens et al., 2016) favoring the transfer of sediment from the Mahanadi watershed to the study site (Dunlea et al., 2020).

Pollen diagram was drawn using Psimpoll 4.25 (Bennett, 2008) (Figures S3 and S9 in Supporting Information S1). Principal Component Analyses (PCA) (Figures S4 and S5 in Supporting Information S1) and calculation of Simpson's diversity Index (Texte S2 in Supporting Information S1) were performed using the *FactoMineR* (Husson et al., 2020) and the *Vegan* (Oksanen et al., 2020) packages respectively with the R software (R Core Team, 2021). The *Astrochton* package (Meyers, 2019) was used to fit a smoothing curve through the data removing low-frequency variations. We used the sample score on the PCA Axis 1 as a humidity index because moisture

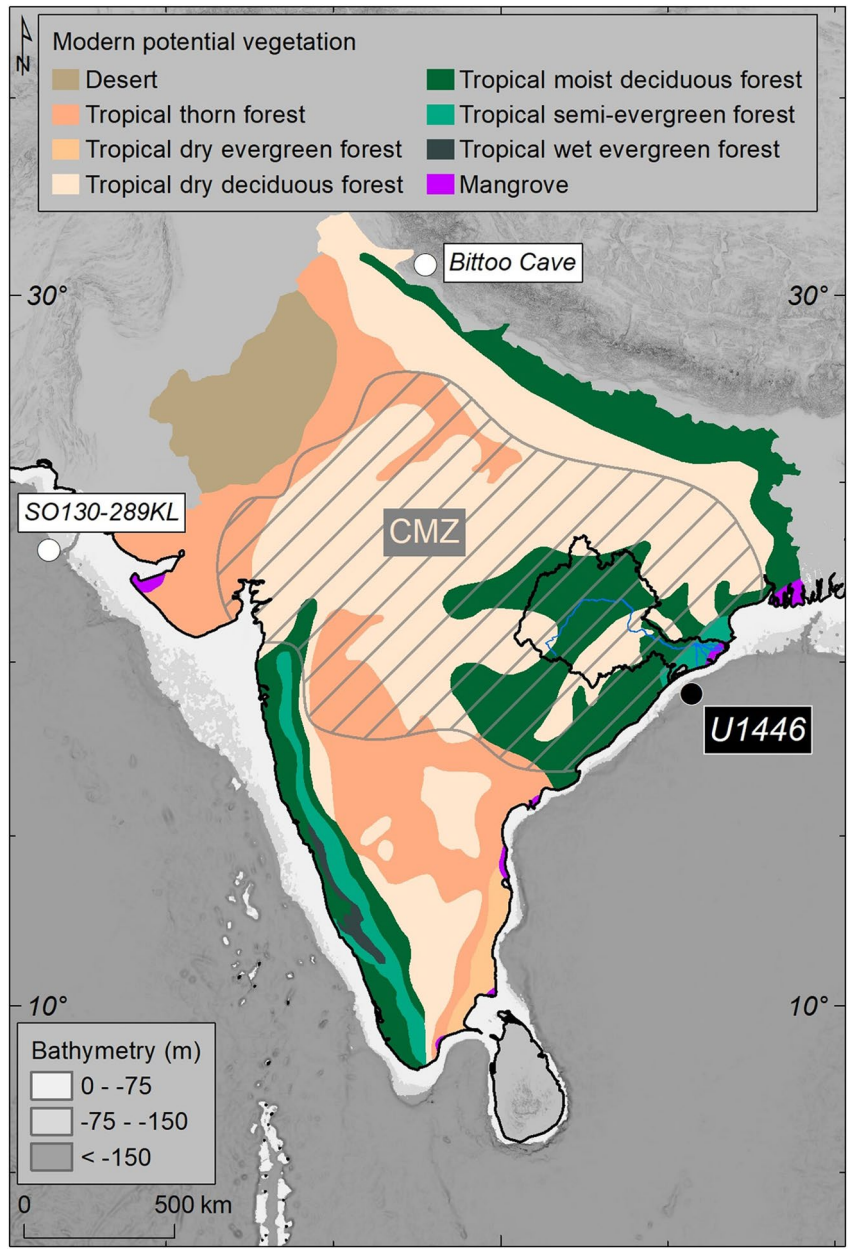

Figure 1. Study site and distribution of modern potential vegetation in Indian Peninsula (modified from Champion & Seth, 1968). The Mahanadi catchment and the Core Monsoon Zone (CMZ) are represented by the blod dark line and the striped area. Location of core SO130-289KL (Deplazes et al., 2014) and record from Bittoo Cave (Kathayat et al., 2016) are also shown.

appears as the main environmental factor controlling the taxa distribution on this axis (Texte S3; Figure S4 in Supporting Information S1).

2.3. Age Model

The age model of the studied section was established using 14 control points, including four ^{14}C dates, the Toba ash layer, two $\delta^{18}O_{benthic}$ dates and four tie points correlating structures in the millennial-scale variability expressed at Site U1446 by calcium content and pollen records to the well-dated $\delta\ ^{18}O_{speletothem}$ in Bittoo Cave (see Texte S1, Figures S1 and S2 in Supporting Information S1, Table S1 in Supporting Information S1). Bayesian age-depth modeling (Figure S1 in Supporting Information S1) was performed with the *BACON* package (Blaauw

& Christen, 2013) in the R environment (R Core Team, 2021). The section of the site corresponding to the last glacial period was subsampled between 6.96 and 16.98 m CCSF-A, representing an average time resolution of ~400 years between 80 and 20 ka, and is composed of dark gray to gray hemipelagic clay with nannofossils and foraminifers (Clemens et al., 2016).

3. Results and Discussion

3.1. Orbital Variations of the Indian Vegetation and Monsoon Rainfall

3.1.1. Vegetation and ISM Changes

The pollen record (Figures 2; S3 in Supporting Information S1) indicates that an open landscape vegetation dominated over the entire glacial period, being composed by emblematic components of the dry subtropical vegetation in southwestern Asia such as the grassland, including Cyperaceae and Poaceae, the semi-arid *Artemisia*, the arid *Ephedra* and the arid and/or halophilous Amaranthaceae (Table S2 in Supporting Information S1; Ansari & Vink, 2007; Davies & Fall 2001; El-Moslimany, 1990; Singh et al., 1973). Given the current vegetation distribution, our pollen results indicate that overall dry conditions and reduced ISM prevailed throughout Marine Isotope Stage (MIS) 5/4 transition to MIS 2, as also suggested by the humidity index (Figure 2).

The widely open vegetation, characterized by the maximum of grassland and the minimum of arboreal taxa recorded during the Last Glacial Maximum (LGM, 23-20 ka), reveals strongly reduced ISM variability in agreement with the lowest levels in the humidity index (Figure 2). During the early MIS 3 (59-42 ka), arboreal taxa and the pollen-derived humidity index reached the highest values (Figure 2). Arboreal taxa, mainly Combretaceae/Melastomataceae, *Glochidion*, *Mallotus* and *Olea paniculata* (Figure 2 and S3 in Supporting Information S1; Champion & Seth, 1968), were important elements of the open to wooded savannah developing in the study area, although probably restricted to the most humid zones of the landscape. Our results clearly indicate that the strongest ISM activity of the last glacial period is achieved during this interval of early MIS 3 (Figure 2). Moreover, it is also noticeable that *Artemisia* became a major element of the herbaceous strata during this interval of intense ISM (Figure 2), suggesting increased moisture availability in winter (Wei et al., 2015). Pollen assemblages during MIS 4 (73-58 ka) and late MIS 3 (42-29 ka) indicate an intermediate expansion of tropical trees, and thus moderate ISM (Figure 2). However, the distinct hydrological preferences of the taxa composing the herbaceous community (Singh et al., 1973) reveal differences in the degree of ISM activity during these two intervals. Hence, the predominance of grasses (Poaceae) at the expense of arid plants (Amaranthaceae) during late MIS 3 suggests moister conditions than during MIS 4, which is further supported by the results of the humidity index (Figures 2, 3 and S3 in Supporting Information S1).

3.1.2. Drivers of Long-Term Indian Vegetation and Monsoon Change

3.1.2.1. ISM Minimum During the LGM

Vegetation changes recorded in the Ganges-Brahmaputra plain (Ghosh et al., 2015) and on the Tibetan Plateau (Zhang et al., 2020) display consistent features with our inferences on rainfall variations during the last glacial period, implying a coherent regional picture of ISM changes at orbital scale. The ISM minimum observed in eastern India at ~22 ka is also consistent with the large-scale drying that affected all the Indian monsoon regions during the LGM (Ansari & Vink, 2007; Van Campo, 1986). This widespread aridification is generally attributed to reduced cross-equatorial transport of atmospheric heat and moisture and to a southward shift in the location of the intertropical convergence zone (ITCZ). Pollen derived-vegetation at Site U1446 supports the inference that the boreal summer ITCZ hardly reached ~20°N, in agreement with its southernmost LGM location in India simulated at ~15°N (Chabangborn et al., 2014). This observation points out that a strong shift of the ITCZ might have occurred during the LGM, regardless of its 1°latitudinal-move estimated at global scale (McGee et al., 2014). Processes related to the topography and albedo of the large LGM ice-sheets are identified as strongly influencing the tropical atmospheric circulation. Ice-sheet feedbacks likely strengthened the conditions favored by low boreal summer insolation forcing (Figure 2) and their growth reduced the global water vapor content of the atmosphere, as well humidity supplied into India (Marzin et al., 2013).

Moreover, we suggest that besides ice-sheet and combined-insolation forcing, regional climatic feedbacks may have also played an important role in amplifying the decrease in tropical forest and ISM strength over the CMZ during the LGM. First, cooling of the Arabian Sea (Anand et al., 2008; Govil & Naidu, 2010) likely played a

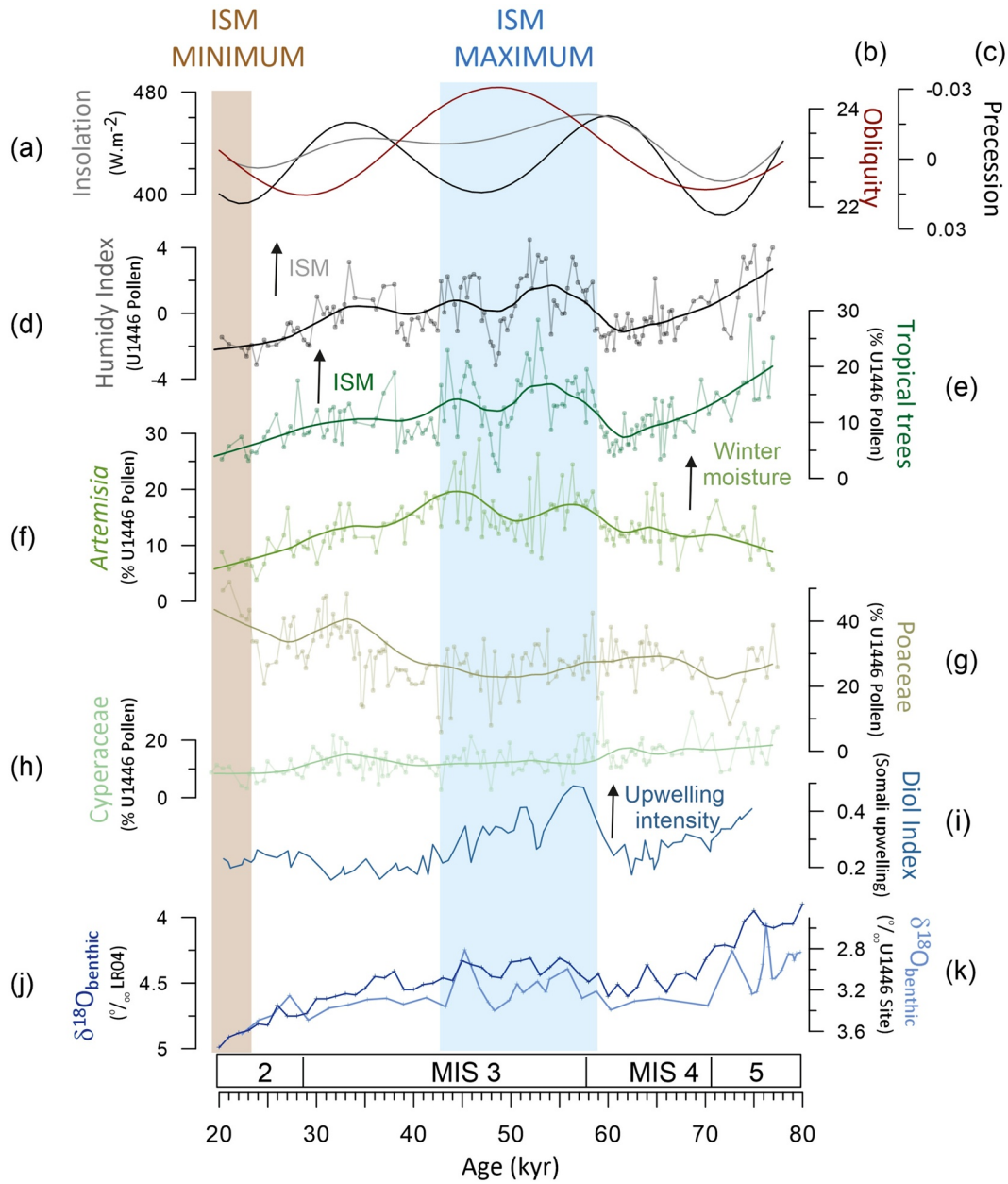

Figure 2. Variations of (a) insolation, (b) obliquity and (c) precession (Laskar et al., 2004) compared with the pollen record at International Ocean Discovery Program Site U1446, including (d) the humidity index, percentages of (e) tropical trees, (f) *Artemisia*, (g) Poaceae and (h) Cyperaceae, with (i) the diol index in the Somali coast (Rampen et al., 2008). At the bottom are represented (j) the $\delta^{18}O_{benthic}$ LRO4 (Lisiecki & Raymo, 2005) and (k) the $\delta^{18}O_{benthic}$ of the study site (McGrath et al., 2021). Orbital maximum and minimum of the Indian Summer Monsoon (ISM) correspond to the blue and brown bands, respectively. Bold lines represent smoothing curves through the pollen data and humidity index.

critical role in amplifying the reduction in ISM rainfall by affecting its nearest moisture source (Cai et al., 2015). Consistently, persistent Westerlies are recorded during the LGM from the Arabian Sea to the Tibetan Plateau, conveying the temperature anomalies from the North Atlantic by tropospheric teleconnection (Kageyama et al., 2009; McGee et al., 2014). Finally, another factor identified as a main feedback mechanism is the low LGM sea-level, which exposes the Sunda and Sahul shelves and excites the Bjerknes feedback (Bjerknes, 1969; Dinezio et al., 2018; Thirumalai et al., 2019). The Bjerknes loop leads to reversed Walker circulation and zonal sea surface temperature gradient in the Indian Ocean reducing regional evaporation, and thus reinforcing the LGM aridity in India.

3.1.2.2. Strong Interhemispheric Thermal Gradient During MIS 3

Both pollen record and humidity index show that the maximum in monsoon rainfall over northeastern Peninsular India during the early MIS 3 interval lags the precession-driven peak in boreal summer insolation by several thousand years (Figure 2). These results add evidence to the complex relationship between boreal summer insolation and ISM variations as pointed out by previous studies in the BoB and the Arabian Sea (Clemens et al., 2021; Govil & Naidu, 2010; Kudrass et al., 2001; Liu et al., 2021; Panmei et al., 2018; Schulz et al., 1998). In contrast, our record disagrees with $\delta^{18}O_{speleothem}$ record from Bittoo Cave, which has been invoked to assert a more direct link between insolation and ISM rainfall (Kathayat et al., 2016). Interpretation of the $\delta^{18}O_{speleothem}$ as a direct indicator of rainfall amount remains an openly debated question, especially for glacial intervals (Clemens et al., 2021; Jasechko et al., 2015).

The MIS 3 monsoon maximum occurs remarkably during an interval marked by in-phase obliquity and precession maxima (Figure 2). Obliquity is a key parameter controlling the intertropical insolation gradient, thereby modulating the cross-equatorial Hadley circulation and the interhemispheric thermal gradient over the Indian Ocean (e.g., Bosmans et al., 2015; Mantsis et al., 2014). The stronger obliquity during the early part of MIS 3 may have increased the pressure contrast between the Southern and the Northern Indian Ocean, reinforcing the heat and moisture transport in the ocean and the atmosphere, which is consistent with the intensification of the Somali upwelling over the interval ~60-45 ka (Rampen et al., 2008, Figure 2). This mechanism likely favored a northward position of the ITCZ and increased the moisture conveyed to India (Beck et al., 2018), a necessary condition for the expansion of a wooded savannah further inland at Site U1446 (Figure 2 and S5 in Supporting Information S1). Moreover, the response of the Asian monsoons to obliquity forcing was likely intensified by low GHGc (Wu & Tsai, 2020).

Although the last glacial pollen record suggests a predominant control of obliquity on ISM intensity during early MIS 3, precession may also have contributed to modify the seasonal hydrological contrast.The increased availability of moisture in winter necessary to sustain the growth of *Artemisia* during this interval may have been triggered by the precession maximum (Figure 2), which counteracts the obliquity maximum and reduces the seasonal constrast. A low precession-induced insolation (i.e., precession maximum) shortens and advances the monsoon season, as well as increases the rainfall during the transitional season (Ding et al., 2021). In addition, warm oceanic conditions recorded in the BoB between 37 and 57 ka (Lauterbach et al., 2020) may also have enhanced the moisture supplied by the winter easterlies or via cyclonic marine influenced storm systems (Wang et al., 2013).

3.2. Abrupt Climatic Events in India

3.2.1. Rapid Vegetation and ISM Changes During the Last Glacial Period

Abrupt and strong landscape openings at ~76-75, 73-72, 61-59, 49-47, 41-39, 30-29 and 26-23 ka, characterized by a large expansion of the arid taxa, such as the halophilous *Amaranthaceae*, constitute the most striking vegetation changes of the last glacial period over the CMZ (Figure 3). Such arid taxa currently spread in modern semi-deserts from Jordan to western China (Davies & Fall 2001; El-Moslimany, 1990; Singh et al., 1973; Zhao et al., 2015) suggest that humidity during these millennial-scale events reached its lowests level of the last glacial period, including the LGM (Figures 2 and 3). We identify these dry events as the response of the ISM to the North Atlantic cold spells (Heinrich, 1988), excepting one at ~73-72 ka, which is likely concurrent to the GI/GS 19 transition (Figure 3).

In contrast to Bittoo Cave (Kathayat et al., 2016), Site U1446 pollen record also provides evidence that individual HSs have variable impacts on vegetation and climate within the CMZ as suggested by the different level of expansion of arid taxa (Figures 3; S6 in Supporting Information S1). The GI/GS 19, HS 5 and HS 2 are characterized by very low ISM magnitude, whereas less intense and dryer conditions are recorded during the HS 7a, 6 and 3. Varying magnitudes of ISM reductions during the HSs seem to be a common feature in marine records from the Arabian Sea to the BoB (e.g., Colin et al., 1998; Deplazes et al., 2014; Lauterbach et al., 2020; Schulte & Müller, 2001). However, so far, no clear apparent pattern emerges from the comparison of the sedimentary records, which may be due to the use of diverse indirect monsoon proxies recording different components of the ISM such as wind, rainfall, runoff, and/or to a complex spatial expression of the amplitude of abrupt ISM changes outside the CMZ. We also acknowledge that geochronological uncertainties during this interval might further

obfuscate coherent patterns of change over this interval. Nevertheless, our records establish that Indian vegetation patterns showed a strong response to millennial-scale ISM changes.

3.2.2. Basic Forcing of the Abrupt ISM Drops

The general increased dryness during the HSs revealed by our pollen record (Figure 3) is wholly consistent with the basin-wide drying documented in all regions of the Indian monsoon subsystem (Figure 3; Deplazes et al., 2014; Lauterbach et al., 2020; Mohtadi et al., 2014; Zorzi et al., 2015). Drier-than-LGM conditions favoring

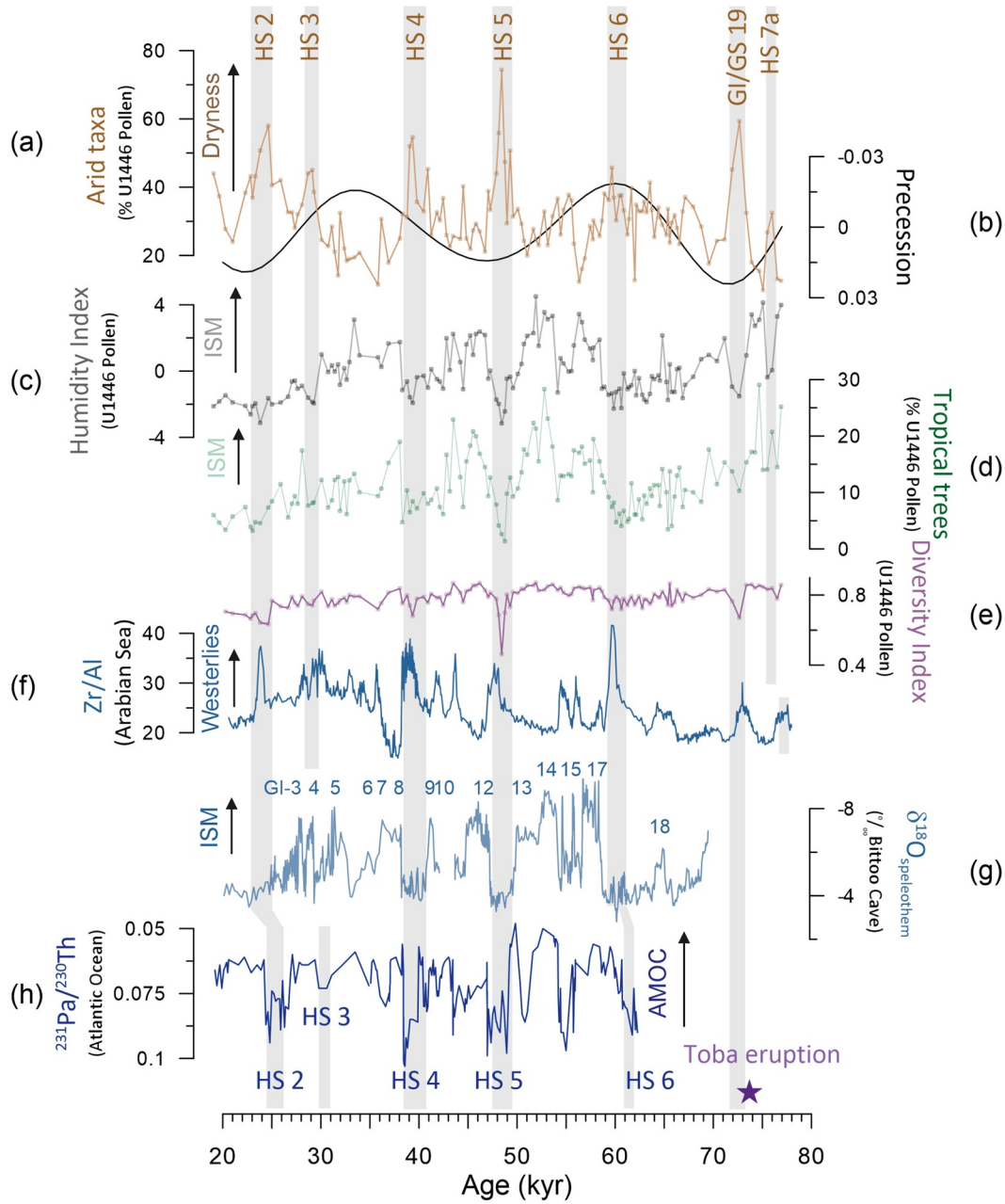

Figure 3. Comparison between millennial-scale variations in (a) arid taxa percentages at International Ocean Discovery Program Site U1446 and (b) precession changes (Laskar et al., 2004). Variations of (c) humidity index, (d) percentages of tropical trees and (e) Simpson's diversity index at the study site are also shown, as well as (f) the Zr/Al ratio from the Arabian Sea (Deplazes et al., 2014), (g) the $\delta^{18}O_{spelothem}$ from Bittoo Cave (Kathayat et al., 2016) and (h) the $^{231}Pa/^{230}Th$ from the North Atlantic (Henry et al., 2016; Lippold et al., 2009). Gray bands represent weak monsoon events.

the expansion of semi-desert vegetation at the expense of grassland are consistent with modeling experiment estimating the HS-ISM average around 220 mm.yr^{-1} (Mohtadi et al., 2014) instead of 280 mm.yr^{-1} during the LGM (Dinezio et al., 2018), which contrast with annual rainfalls varying between 1,300 and 1,500 mm.yr^{-1} in the Mahanadi catchment during the 1975–2010 interval (Beck et al., 2005). Proxy and models showed that the large-scale weakening of the ISM results from the reorganization of the Hadley circulation over the entire realm of the Indian Ocean in response to the abrupt cooling event in the North Atlantic and associated Atlantic meridional overturning circulation (AMOC) changes (Mohtadi et al., 2014). This reorganization implies a marked decrease in interhemispheric moisture transport and a stronger-than-LGM southward shift of the ITCZ allowing in turn, a humidity increase in southern Indonesia and northern Australia (Mohtadi et al., 2014). In addition, the Northern Hemisphere cold spells likely propagated to the Arabian Sea with strengthened northwesterly winds generating dynamically important sea surface cooling (Figure 3; e.g., Deplazes et al., 2014; Schulte & Müller, 2001). The cooling in the Arabian Sea likely contributed to reduced monsoon rainfall in India as the ISM appears to be extremely sensitive to the Arabian Sea surface temperatures (Borah et al., 2020; Tierney et al., 2016).

The event at the GI/GS 19 transition detected at Site U1446 (Figure 3) correlates well with a severe shift in the Indian hydroclimate (Black et al., 2021). The large explosive eruption of the Toba volcano ∼74 ka (Crick et al., 2021) has been invoked as a cause for this major drying event in India, despite the moderate cooling recorded in the North Atlantic (Kindler et al., 2014) and muted signal of positive Westerlies anomaly in the Arabian Sea (Figure 3; Deplazes et al., 2014). Large northern hemisphere volcanic eruptions can generate a global southward shift of the ITCZ by increasing atmospheric aerosol concentration (Ridley et al., 2015) and therefore reduce the ISM rainfall.

3.2.3. Potential Influence of High Latitude Forcing Diversity

Variations in both amount and regional source of iceberg discharges have palyed a major role in changing the amplitude of AMOC slowdown and global temperature change patterns (Henry et al., 2016; Roche et al., 2010), potentially impacting the intensity of the ISM to a greater or lesser extent depending on the HS considered. Noticeably, the millennial events characterized by least intense drought conditions at Site U1446, the HS 3 and 6, coincide with Fennoscandian ice-sheet surges, whereas the driest episodes, the HS 5 and 2, occur at the time of the Laurentide ice-sheet iceberg discharges (Grousset et al., 1993; Hemming, 2004), suggesting that the latter exerts a stronger control on Indian sub-continent aridity. However, this observation disagrees with a modeling experiment showing that the different origin of the freshwater pulses causes distinct regional responses in the North Atlantic Ocean but no impact is detected in the Indian Ocean (Roche et al., 2010). We hypothesize that the main cause of these data-model discrepancies is linked to the absence of the height of the Laurentide ice-sheet in the model that only includes the freshwater input. As demonstrated by previous work (Roberts et al., 2014), the height of this ice-sheet significantly affects tropical regions through a reorganization of the atmospheric circulation that favors the transfer of North Atlantic atmospheric anomalies to India during Laurentide iceberg discharges.

3.2.4. Modulation of the Abrupt ISM Drop by Precession

The GI/GS 19, HS 5 and 2 are exceptionally expressed in our pollen-derived Indian vegetation record, although they are not the most pronounced in the North Atlantic region where the largest iceberg release resulting in the strongest AMOC reduction is recorded during the HS 4 (Figure 3; Lisiecki & Stern, 2016). A noticeable common feature between the driest Indian events lies in their phasing with a precession maximum, that is, when Earth is at aphelion during summer (Figure 3). In these astronomical contexts, the thermal seasonal contrast in India is reduced, decreasing the ISM strengh (Mohtadi et al., 2016). We suggest that the precession-induced low boreal summer insolation enhanced the unfavorable atmospheric and oceanographic reoganizations associated with the iceberg surge events in the North Atlantic, as well as the effect of the volcanic eruption for the GI/GS19.

The hypothesis that the interconnection between orbital and millennial forcings acted on the amplitude of abrupt changes in the EASM has been proposed to explain the $\delta^{18}O_{speleothem}$ record (Cheng et al., 2016), and it has been recently challenged by Thirumalai et al. (2020). More recently, a new study based on a microcodium $\delta^{18}O$ record from the Chinese Loess Plateau, almost exclusively influenced by summer precipitation, shows a larger amplitude of millennial-scale EASM variability during precession maximum, and hence the boreal summer insolation

minima of the last glacial period (Zhang et al., 2022). Thus, it is likely that modulation of the millennial-scale variability by precession is also operating in the ISM subsystem at least during the most dramatic weak monsoon events of the last glacial period, as we observe in vegetation dynamics.

3.3. Lessons From the Past?

While recent global change undeniably affects biodiversity (Nunez et al., 2019), how resilient has Indian vegetation been to the orbital and millennial climate variations observed in this study? The Simpson index, classically used to measure biological diversity, remains stable at the orbital scale, but decreases during the abrupt arid events (Figure 3). Although relationship between past and modern tropical vegetation diversity is difficult to assess using pollen records (Gosling et al., 2018), systematic decrease in pollen diversity during past extreme weak ISM events is consistent with lower specific richness of open vegetation relative to forest environments (Box & Fujiwara, 2013; Sankaran & Ratnam, 2013). Hence, our study points out the strong sensitivity of the northern Peninsular Indian ecosystem to ISM changes and in particular to abrupt events. Nonetheless, the glacial pollen record also shows the resilience of vegetation to intense hydrological stress that should therefore be considered to better anticipate changes associated to future abrupt hydrological shifts in (sub)tropical dry environments.

In addition, we suggested that phasing between precession maxima and the North Atlantic icebergs discharges led to reduced-ISM during the last glacial period. In the framework of low precession (Laskar et al., 2004), this suggestion makes questionable the impact of the ongoing Arctic melting on the recurrence and intensity of recently recorded extreme events in India (Mishra, 2020; Mishra et al., 2021). The study of Indian vegetation and monsoonal changes during the last glaciation thus offers important lessons about the response of subtropical ecosystems shiting from savannah to semi-desert environments, and hydroclimate variabilities, even though we are moving toward a warmer and wetter world with different boundary conditions.

4. Conclusions

Pollen-derived vegetation reconstructions from the IODP Site U1446 provide a robust, millennial-scale resolution record of Indian hydroclimate variability through the ~80-20 ka interval. Our pollen record reveals an open tropical landscape with sparse tree cover in eastern India, driven by reduced summer monsoon precipitation during the last glacial period. We propose that the humidity maximum recorded during the early portion of MIS 3 results from a suitable in-phase orbital configuration between obliquity and precession maxima, which likely favors a strong interhemispheric thermal contrast leading to increased heat and moisture supplies across the Indian Ocean. Drier conditions during the HSs relative to the LGM might result from a superimposed slowdown of the AMOC, reinforcing the cooling of the Arabian Sea and subsequent dynamical impact on the ISM intensity. Finally, one of the major findings of our work was to document for the first time a modulated and regional expression of the ISM to the distinctive HSs. Unless a stronger response of the ISM to the Laurentide ice-sheet surges is recorded, our study shows a non-linear relationship between the magnitude of the AMOC slowdowns due to the amount of icebergs releases, and the magnitude of Indian vegetation and hydroclimate changes. We propose that the ISM millennial-scale variability is strongly influenced by the orbital context, specifically by precession-induced insolation changes.

Data Availability Statement

The International Ocean Discovery Program Site U1446 pollen data used for reconstructing vegetation and monsoon changes in India during the last glacial period is available in the Pangaea Repository under the https://doi.org/10.1594/PANGAEA.946372.

Acknowledgments
Financial support was provided by the Ecole Pratique des Hautes Etudes (EPHE) to CZ and by the French research program INSU LEFE and International Ocean Discovery Program (IODP) France to PM. KT acknowledges support from the University of Arizona Technology and Research Initiative Fund (TRIF) and support from NSF grant #AGS2103077. DO acknowledges funding from FCT through INDRA project (EXPL/CTA-CLI/0612/2021), CCMAR FCT Research Unit-project UIDB/04326/2020 and contract (CEECIND/02208/2017). The authors are grateful to the chief-scientists Steven Clemens, Wolfgang Kuhnt, the staff scientist Leah Levay, the technical staff and crews of IODP expedition 353 "Indian Monsoon Rainfall," the IODP Kochi Core Curation staff for their efforts in providing the samples used in this study. We warmly thank Ludovic Devaux for the palynological lab preparation, Vincent Hanquiez for modifying the modern potential vegetation map. We are also thankful to the Museum National d'Histoire Naturelle (MNHN) and to the Observatoire de REcherche Méditerranéen de l'Environnement (OSU OREME) for providing access to the palynological reference collection, as well to Dr Thierry Deroin, curator at the MNHN, who supported our request. CZ warmly thanks the French associations Association des Palynologues de Langue Française (APLF) and Association Française pour l'Étude du Quaternaire – Comité National Français de l'International Quaternary Association (AFEQ-CNF-INQUA) for providing the financial support to present this study at the AGU fall meeting 2021.

References

Anand, P., Kroon, D., Singh, A. D., Ganeshram, R. S., Ganssen, G., & Elderfield, H. (2008). Coupled sea surface temperature–seawater δ18O reconstructions in the Arabian Sea at the millennial scale for the last 35 ka. *Paleoceanography*, *23*(4). https://doi.org/10.1029/2007PA001564

Ansari, M. H., & Vink, A. (2007). Vegetation history and palaeoclimate of the past 30 kyr in Pakistan as inferred from the palynology of continental margin sediments off the Indus Delta. *Review of Palaeobotany and Palynology*, *145*(3–4), 201–216. https://doi.org/10.1016/j.revpalbo.2006.10.005

Bastia, F., & Equeenuddin, S. M. (2016). Spatio-temporal variation of water flow and sediment discharge in the Mahanadi River, India. *Global and Planetary Change*, *144*, 51–66. https://doi.org/10.1016/j.gloplacha.2016.07.004

Beck, C., Grieser, J., & Rudolf, B. (2005). A new monthly precipitation climatology for the global land areas for the period 1951 to 2000. *Geophysical Research Abstracts*, *7*, 07154.

Beck, J. W., Zhou, W., Li, C., Wu, Z., White, L., Xian, F., et al. (2018). A 550, 000-year record of East Asian monsoon rainfall from 10Be in loess. *Science*, *360*(6391), 877–881. https://doi.org/10.1126/science.aam5825

Bennett, K. (2008). *Psimpoll and Pscomb software*. Queen's University Belfast.

Bjerknes, J. (1969). Atmospheric teleconnections from the equatorial Pacific. *Monthly Weather Review*, *97*(3), 163–172. https://doi.org/10.1175/1520-0493(1969)097<0163:ATFTEP>2.3.CO;2

Blaauw, M., & Christen, J. A. (2013). Bacon manual V2. 3.3. Retrieved from http://www.chrono.qub.ac.uk/blaauw/bacon.html

Black, B. A., Lamarque, J.-F., Marsh, D. R., Schmidt, A., & Bardeen, C. G. (2021). Global climate disruption and regional climate shelters after the Toba supereruption. *Proceedings of the National Academy of Sciences*, *118*(29). https://doi.org/10.1073/pnas.201304611

Blasco, F., Bellan, M. F., & Aizpuru, M. (1996). A vegetation map of tropical continental Asia at scale 1:5 million. *Journal of Vegetation Science*, *7*(5), 623–634. https://doi.org/10.2307/3236374

Blasco, F., Whitmore, T. C., & Gers, C. (2000). A framework for the worldwide comparison of tropical woody vegetation types. *Biological Conservation*, *95*(2), 175–189. https://doi.org/10.1016/S0006-3207(00)00032-X

Borah, P. J., Venugopal, V., Sukhatme, J., Muddebihal, P., & Goswami, B. N. (2020). Indian monsoon derailed by a North Atlantic wavetrain. *Science*, *370*(6522), 1335–1338. https://doi.org/10.1126/science.aay6043

Bosmans, J. H. C., Hilgen, F. J., Tuenter, E., & Lourens, L. J. (2015). Obliquity forcing of low-latitude climate. *Climate of the Past*, *11*(10), 1335–1346. https://doi.org/10.5194/cp-11-1335-2015

Box, E. O., & Fujiwara, K. (2013). In *Asia, ecosystems of. Encyclopedia of biodiversity* (2nd ed., pp. 254–280). https://doi.org/10.1016/B978-0-12-384719-5.00304-X

Cai, Y., Fung, I. Y., Edwards, R. L., An, Z., Cheng, H., Lee, J.-E., et al. (2015). Variability of stalagmite-inferred Indian monsoon precipitation over the past 252, 000 y. *Proceedings of the National Academy of Sciences of the United States of America*, *112*(10), 2954–2959. https://doi.org/10.1073/pnas.1424035112

Chabangborn, A., Brandefelt, J., & Wohlfarth, B. (2014). Asian monsoon climate during the last glacial maximum: Palaeo-data–model comparisons. *Boreas*, *43*(1), 220–242. https://doi.org/10.1111/bor.12032

Champion, S. H. G., & Seth, S. K. (1968). A revised Survey of the forest Types of India.

Cheng, H., Edwards, R. L., Sinha, A., Spötl, C., Yi, L., Chen, S., et al. (2016). The Asian monsoon over the past 640, 000 years and ice age terminations. *Nature*, *534*(7609), 640–646. https://doi.org/10.1038/nature18591

Clemens, S. C., Kuhnt, W., & LeVay, L. J. (2016). Expedition 353 scientists. *Proceedings of the International Ocean Discovery Program*, *353*. https://doi.org/10.14379/iodp.proc.353.2016

Clemens, S. C., & Prell, W. L. (2003). A 350, 000 year summer-monsoon multi-proxy stack from the Owen ridge, northern Arabian Sea. *Marine Geology, Asian Monsoons and Global Linkages on Milankovitch and Sub-Milankovitch Time Scales*, *201*(1–3), 35–51. https://doi.org/10.1016/S0025-3227(03)00207-X

Clemens, S. C., Yamamoto, M., Thirumalai, K., Giosan, L., Richey, J. N., Nilsson-Kerr, K., et al. (2021). Remote and local drivers of Pleistocene South Asian summer monsoon precipitation: A test for future predictions. *Science Advances*, *7*(23), eabg3848. https://doi.org/10.1126/sciadv.abg3848

Colin, C., Kissel, C., Blamart, D., & Turpin, L. (1998). Magnetic properties of sediments in the Bay of bengal and the Andaman sea: Impact of rapid North Atlantic ocean climatic events on the strength of the Indian monsoon. *Earth and Planetary Science Letters*, *160*(3–4), 623–635. https://doi.org/10.1016/S0012-821X(98)00116-2

Corrick, E. C., Drysdale, R. N., Hellstrom, J. C., Capron, E., Rasmussen, S. O., Zhang, X., et al., (2020). Synchronous timing of abrupt climate changes during the last glacial period. https://doi.org/10.17863/CAM.56908

Crick, L., Burke, A., Hutchison, W., Kohno, M., Moore, K. A., Savarino, J., et al. (2021). New insights into the ∼74 ka Toba eruption from sulfur isotopes of polar ice cores. *Atmospheric Dynamics/Ice Cores/Pleistocene*. https://doi.org/10.5194/cp-2021-38

Davies, C. P., & Fall, P. L. (2001). Modern pollen precipitation from an elevational transect in central Jordan and its relationship to vegetation. *Journal of Biogeography*, *28*(10), 1195–1210. https://doi.org/10.1046/j.1365-2699.2001.00630.x

Deplazes, G., Lückge, A., Stuut, J.-B. W., Pätzold, J., Kuhlmann, H., Husson, D., et al. (2014). Weakening and strengthening of the Indian monsoon during Heinrich events and Dansgaard-Oeschger oscillations. *Paleoceanography*, *29*(2), 99–114. https://doi.org/10.1002/2013PA002509

Dinezio, P., Tierney, J., Otto-Bliesner, B., Timmermann, A., Bhattacharya, T., Rosenbloom, N., & Brady, E. (2018). Glacial changes in tropical climate amplified by the Indian Ocean. *Science Advances*, *4*(12), eaat9658. https://doi.org/10.1126/sciadv.aat9658

Ding, Z., Huang, G., Liu, F., Wu, R., & Wang, P. (2021). Responses of global monsoon and seasonal cycle of precipitation to precession and obliquity forcing. *Climate Dynamics*, *56*(11–12), 3733–3747. https://doi.org/10.1007/s00382-021-05663-6

Dunlea, A. G., Giosan, L., & Huang, Y. (2020). Pliocene expansion of C4 vegetation in the core monsoon zone on the Indian Peninsula. *Climate of the Past*, *16*(6), 2533–2546. https://doi.org/10.5194/cp-16-2533-2020

El-Moslimany, A. P. (1990). Ecological significance of common nonarboreal pollen: Examples from drylands of the Middle East. Review of Palaeobotany and palynology. *The Proceedings of the 7th International Palynological Congress (Part I)*, *64*, 343–350. https://doi.org/10.1016/0034-6667(90)90150-H

Gaussen, H., Meher-Homji, V. M., Blasco, F., Deleccurt, A., Foutannel, J., Legris, P., & Troy, J. P. (1973). International map of vegetation and environmental conditions, sheet: Orissa. *Fr. Pondichery. Tr. Sect. Sci. Tech. Hors. Series*, *71*(14).

Ghosh, R., Bera, S., Sarkar, A., Paruya, D. K., Yao, Y.-F., & Li, C.-S. (2015). A ∼50 ka record of monsoonal variability in the Darjeeling foothill region, eastern Himalayas. *Quaternary Science Reviews*, *114*, 100–115. https://doi.org/10.1016/j.quascirev.2015.02.002

Gosling, W. D., Julier, A. C. M., Adu-Bredu, S., Djagbletey, G. D., Fraser, W. T., Jardine, P. E., et al. (2018). Pollen-vegetation richness and diversity relationships in the tropics. *Vegetation History and Archaeobotany*, *27*(2), 411–418. https://doi.org/10.1007/s00334-017-0642-y

Govil, P., & Naidu, P. D. (2010). Evaporation-precipitation changes in the eastern Arabian Sea for the last 68 ka: Implications on monsoon variability. *Paleoceanography*, *25*(1). https://doi.org/10.1029/2008PA001687

Grousset, F., Labeyrie, L., Sinko, J., Cremer, M., Bond, G., Duprat, J., et al. (1993). Patterns of ice-Rafted detritus in the glacial North Atlantic (40–55°N). *Paleoceanography*, *8*(2), 175–192. https://doi.org/10.1029/92PA02923

Gupta, A. K., Anderson, D. M., Pandey, D. N., & Singhvi, A. K. (2006). Adaptation and human migration, and evidence of agriculture coincident with changes in the Indian summer monsoon during the Holocene. *Current Science*, *90*, 1082–1090.

Heinrich, H. (1988). Origin and Consequences of cyclic ice Rafting in the Northeast Atlantic Ocean during the past 130, 000 Years. *Quaternary Research*, *29*(2), 142–152. https://doi.org/10.1016/0033-5894(88)90057-9

Hemming, S. R. (2004). Heinrich events: Massive late pleistocene detritus layers of the North Atlantic and their global climate imprint. *Reviews of Geophysics*, *42*, 1–43. https://doi.org/10.1029/2003RG000128

Henry, L. G., McManus, J. F., Curry, W. B., Roberts, N. L., Piotrowski, A. M., & Keigwin, L. D. (2016). North Atlantic ocean circulation and abrupt climate change during the last glaciation. *Science*, *353*(6298), 470–474. https://doi.org/10.1126/science.aaf5529

Husson, F., Josse, J., Le, S., & Mazet, J. (2020). FactoMineR: Multivariate exploratory data analysis and data mining.

Jasechko, S., Lechler, A., Pausata, F. S. R., Fawcett, P. J., Gleeson, T., Cendón, D. I., et al. (2015). Late-glacial to late-Holocene shifts in global precipitation $\delta^{18}O$. *Climate of the Past*, *11*(10), 1375–1393. https://doi.org/10.5194/cp-11-1375-2015

Kageyama, M., Mignot, J., Swingedouw, D., Marzin, C., Alkama, R., & Marti, O. (2009). Glacial climate sensitivity to different states of the Atlantic meridional overturning circulation: Results from the IPSL model. *Climate of the Past*, *5*(3), 551–570. https://doi.org/10.5194/cp-5-551-2009

Kathayat, G., Cheng, H., Sinha, A., Spötl, C., Edwards, R. L., Zhang, H., et al. (2016). Indian monsoon variability on millennial-orbital timescales. *Scientific Reports*, *6*(1), 24374. https://doi.org/10.1038/srep24374

Katzenberger, A., Schewe, J., Pongratz, J., & Levermann, A. (2021). Robust increase of Indian monsoon rainfall and its variability under future warming in CMIP6 models. *Earth System Dynamics*, *12*(2), 367–386. https://doi.org/10.5194/esd-12-367-2021

Kindler, P., Guillevic, M., Baumgartner, M., Schwander, J., Landais, A., & Leuenberger, M. (2014). Temperature reconstruction from 10 to 120 kyr b2k from the NGRIP ice core. *Climate of the Past*, *10*(2), 887–902. https://doi.org/10.5194/cp-10-887-2014

Kudrass, H. R., Hofmann, A., Doose, H., Emeis, K., Erlenkeuser, H. (2001). Modulation and amplification of climatic changes in the Northern Hemisphere by the Indian summer monsoon during the past 80 k.y. *Geology*, *29*, 63–66. https://doi.org/10.1130/0091-7613(2001)029<0063:MAAOCC>2.0.CO;2

Laskar, J., Robutel, P., Joutel, F., Gastineau, M., Correia, A. C. M., & Levrard, B. (2004). A long-term numerical solution for the insolation quantities of the Earth. *A&A*, *428*(1), 261–285. https://doi.org/10.1051/0004-6361:20041335

Lauterbach, S., Andersen, N., Wang, Y. V., Blanz, T., Larsen, T., & Schneider, R. R. (2020). An 130 kyr record of surface water temperature and δ18O from the northern Bay of bengal: Investigating the Linkage Between Heinrich Events and Weak Monsoon Intervals in Asia. *Paleoceanography and Paleoclimatology*, *35*(2), e2019PA003646. https://doi.org/10.1029/2019PA003646

Lippold, J., Grützner, J., Winter, D., Lahaye, Y., Mangini, A., & Christl, M. (2009). Does sedimentary 231Pa/230Th from the Bermuda Rise monitor past Atlantic meridional overturning circulation? *Geophysical Research Letters*, *36*(12), L12601. https://doi.org/10.1029/2009GL038068

Lisiecki, L. E., & Raymo, M. E. (2005). A Pliocene-Pleistocene stack of 57 globally distributed benthic δ18O records. *Paleoceanography*, *20*(1). https://doi.org/10.1029/2004PA001071

Lisiecki, L. E., & Stern, J. V. (2016). Regional and global benthic δ18O stacks for the last glacial cycle. *Paleoceanography*, *31*(10), 1368–1394. https://doi.org/10.1002/2016PA003002

Liu, S., Ye, W., Chen, M.-T., Pan, H.-J., Cao, P., Zhang, H., et al. (2021). Millennial-scale variability of Indian summer monsoon during the last 42 kyr: Evidence based on foraminiferal Mg/Ca and oxygen isotope records from the central Bay of Bengal. *Palaeogeography, Palaeoclimatology, Palaeoecology*, *562*, 110112. https://doi.org/10.1016/j.palaeo.2020.110112

Mantsis, D. F., Lintner, B. R., Broccoli, A. J., Erb, M. P., Clement, A. C., & Park, H. S. (2014). The response of large-scale circulation to obliquity-induced changes in meridional heating gradients. *Journal of Climate*, *27*(14), 5504–5516. https://doi.org/10.1175/JCLI-D-13-00526.1

Marzin, C., Kallel, N., Kageyama, M., Duplessy, J.-C., & Braconnot, P. (2013). Glacial fluctuations of the Indian monsoon and their relationship with North Atlantic climate: New data and modelling experiments. *Climate of the Past*, *9*(5), 2135–2151. https://doi.org/10.5194/cp-9-2135-2013

McGee, D., Donohoe, A., Marshall, J., & Ferreira, D. (2014). Changes in ITCZ location and cross-equatorial heat transport at the last glacial maximum, Heinrich Stadial 1, and the mid-Holocene. *Earth and Planetary Science Letters*, *390*, 69–79. https://doi.org/10.1016/j.epsl.2013.12.043

McGrath, S. M., Clemens, S. C., Huang, Y., & Yamamoto, M. (2021). Greenhouse gas and ice volume drive pleistocene Indian summer monsoon precipitation isotope variability. *Geophysical Research Letters*, *48*(4), e2020GL092249. https://doi.org/10.1029/2020GL092249

Meyers, S. R. (2019). Cyclostratigraphy and the problem of astrochronologic testing. *Earth-Science Reviews*, *190*, 190–223. https://doi.org/10.1016/j.earscirev.2018.11.015

Mishra, V. (2020). Long-term (1870–2018) drought reconstruction in context of surface water security in India. *Journal of Hydrology*, *580*, 124228. https://doi.org/10.1016/j.jhydrol.2019.124228

Mishra, V., Thirumalai, K., Jain, S., & Aadhar, S. (2021). Unprecedented drought in South India and recent water scarcity. *Environmental Research Letters*, *16*(5), 054007. https://doi.org/10.1088/1748-9326/abf289

Mohtadi, M., Prange, M., Oppo, D. W., De Pol-Holz, R., Merkel, U., Zhang, X., et al. (2014). North Atlantic forcing of tropical Indian Ocean climate. *Nature*, *509*(7498), 76–80. https://doi.org/10.1038/nature13196

Mohtadi, M., Prange, M., & Steinke, S. (2016). Palaeoclimatic insights into forcing and response of monsoon rainfall. *Nature*, *533*(7602), 191–199. https://doi.org/10.1038/nature17450

Nunez, S., Arets, E., Alkemade, R., Verwer, C., & Leemans, R. (2019). Assessing the impacts of climate change on biodiversity: Is below 2°C enough? *Climatic Change*, *154*(3–4), 351–365. https://doi.org/10.1007/s10584-019-02420-x

Oksanen, J., Blanchet, F. G., Friendly, M., Kindt, R., Legendre, P., McGlinn, D., et al., (2020). vegan: Community Ecology package.

Panmei, C., Naidu, P. D., & Naik, S. S. (2018). Variability of terrigenous input to the Bay of Bengal for the last ∼80 kyr: Implications on the Indian monsoon variability. *Geo-Marine Letters*, *38*(4), 341–350. https://doi.org/10.1007/s00367-018-0538-6

Prell, W. L., & Kutzbach, J. E. (1992). Sensitivity of the Indian monsoon to forcing parameters and implications for its evolution. *Nature*, *360*(6405), 647–652. https://doi.org/10.1038/360647a0

Rampen, S. W., Schouten, S., Koning, E., Brummer, G.-J. A., & Sinninghe Damsté, J. S. (2008). A 90 kyr upwelling record from the northwestern Indian Ocean using a novel long-chain diol index. *Earth and Planetary Science Letters*, *276*(1–2), 207–213. https://doi.org/10.1016/j.epsl.2008.09.022

Ratnam, J., Bond, W. J., Fensham, R. J., Hoffmann, W. A., Archibald, S., Lehmann, C. E. R., et al. (2011). When is a "forest" a savanna, and why does it matter? *Global Ecology and Biogeography*, *20*(5), 653–660. https://doi.org/10.1111/j.1466-8238.2010.00634.x

Ratnam, J., Sheth, C., & Sankaran, M. (2019). African and Asian savannas. In *Savanna woody plants and large herbivores* (pp. 25–49). John Wiley & Sons, Ltd. https://doi.org/10.1002/9781119081111.ch2

Ratnam, J., Tomlinson, K. W., Rasquinha, D. N., & Sankaran, M. (2016). Savannahs of Asia: Antiquity, biogeography, and an uncertain future. *Philosophical Transactions of the Royal Society B: Biological Sciences*, *371*(1703), 20150305. https://doi.org/10.1098/rstb.2015.0305

R Core Team. (2021). *R: A language and environment for statistical computing*. R Foundation for Statistical Computing. URL Retrieved from https://www.R-project.org/

Ridley, H. E., Asmerom, Y., Baldini, J. U. L., Breitenbach, S. F. M., Aquino, V. V., Prufer, K. M., et al. (2015). Aerosol forcing of the position of the intertropical convergence zone since ad 1550. *Nature Geoscience*, *8*(3), 195–200. https://doi.org/10.1038/ngeo2353

Riedel, N., Fuller, D. Q., Marwan, N., Poretschkin, C., Basavaiah, N., Menzel, P., et al. (2021). Monsoon forced evolution of savanna and the spread of agro-pastoralism in peninsular India. *Scientific Reports*, *11*(1), 9032. https://doi.org/10.1038/s41598-021-88550-8

Roberts, W. H. G., Valdes, P. J., & Payne, A. J. (2014). Topography's crucial role in Heinrich Events. *Proceedings of the National Academy of Sciences*, *111*(47), 16688–16693. https://doi.org/10.1073/pnas.1414882111

Roche, D. M., Wiersma, A. P., & Renssen, H. (2010). A systematic study of the impact of freshwater pulses with respect to different geographical locations. *Climate Dynamics*, *34*(7–8), 997–1013. https://doi.org/10.1007/s00382-009-0578-8

Sánchez-Goñi, M. F., Desprat, S., Fletcher, W. J., Morales-Molino, C., Naughton, F., Oliveira, D., et al. (2018). Pollen from the Deep-sea: A breakthrough in the Mystery of the ice ages. *Frontiers of Plant Science*, *9*. https://doi.org/10.3389/fpls.2018.00038. https://www.frontiersin.org/article/10.3389/fpls.2018.00038

Sankaran, M., & Ratnam, J. (2013). African and Asian savannas. In S. A. Levin (Ed.), *Encyclopedia of biodiversity* (2nd ed., pp. 58–74). Academic Press. https://doi.org/10.1016/B978-0-12-384719-5.00355-5

Schulte, S., & Müller, P. J. (2001). Variations of sea surface temperature and primary productivity during Heinrich and Dansgaard-Oeschger events in the northeastern Arabian Sea. *Geo-Marine Letters*, *21*(3), 168–175. https://doi.org/10.1007/s003670100080

Schulz, H., von Rad, U., Erlenkeuser, H., & von Rad, U. (1998). Correlation between Arabian Sea and Greenland climate oscillations of the past 110, 000 years. *Nature*, *393*(6680), 54–57. https://doi.org/10.1038/31750

Shaw, R., Luo, Y., Cheong, T. S., Abdul Halim, S., Chaturvedi, S., Hashizume, M., et al. (2022). Asia. In H.-O. Pörtner, D. C. Roberts, M. Tignor, E. S. Poloczanska, K. Mintenbeck, A. Alegría, et al. (Eds.), *Climate change 2022: Impacts, adaptation, and Vulnerability.Contribution of working group II to the sixth assessment report of the intergovernmental panel on climate change*. Cambridge University Press.

Singh, G., Chopra, S. K., & Singh, A. B. (1973). Pollen-Rain from the vegetation of North-west India. *New Phytologist*, *72*(1), 191–206. https://doi.org/10.1111/j.1469-8137.1973.tb02025.x

Tharammal, T., Bala, G., Paul, A., Noone, D., Contreras-Rosales, A., & Thirumalai, K. (2021). Orbitally driven evolution of Asian monsoon and stable water isotope ratios during the Holocene: Isotope-enabled climate model simulations and proxy data comparisons. *Quaternary Science Reviews*, *252*, 106743. https://doi.org/10.1016/j.quascirev.2020.106743

Thirumalai, K., Clemens, S. C., & Partin, J. W. (2020). Methane, monsoons, and modulation of millennial-scale climate. *Geophysical Research Letters*, *47*(9), e2020GL087613. https://doi.org/10.1029/2020GL087613

Thirumalai, K., DiNezio, P. N., Tierney, J. E., Puy, M., & Mohtadi, M. (2019). An El Niño Mode in the glacial Indian ocean? *Paleoceanography and Paleoclimatology*, *34*(8), 1316–1327. https://doi.org/10.1029/2019PA003669

Tierney, J. E., Pausata, F. S. R., & de Menocal, P. (2016). Deglacial Indian monsoon failure and North Atlantic stadials linked by Indian Ocean surface cooling. *Nature Geoscience*, *9*(1), 46–50. https://doi.org/10.1038/ngeo2603

Van Campo, E. (1986). Monsoon fluctuations in two 20, 000-yr B.P. Oxygen-Isotope/Pollen records off southwest India 1. *Quaternary Research*, *26*(3), 376–388. https://doi.org/10.1016/0033-5894(86)90097-9

Wang, S.-Y., Buckley, B. M., Yoon, J.-H., & Fosu, B. (2013). Intensification of premonsoon tropical cyclones in the Bay of Bengal and its impacts on Myanmar. *Journal of Geophysical Research: Atmospheres*, *118*(10), 4373–4384. https://doi.org/10.1002/jgrd.50396

Wei, H., Fan, Q., Zhao, Y., Ma, H., Shan, F., An, F., & Yuan, Q. (2015). A 94–10ka pollen record of vegetation change in Qaidam Basin, northeastern Tibetan Plateau. *Palaeogeography, Palaeoclimatology, Palaeoecology*, *431*, 43–52. https://doi.org/10.1016/j.palaeo.2015.04.025

Wu, C.-H., & Tsai, P.-C. (2020). Obliquity-driven changes in east Asian seasonality. *Global and Planetary Change*, *189*, 103161. https://doi.org/10.1016/j.gloplacha.2020.103161

Yan, L., Liu, X., Yang, P., Yin, Z.-Y., & North, G. R. (2011). Study of the impact of summer monsoon circulation on spatial distribution of aerosols in east Asia based on numerical simulations. *Journal of Applied Meteorology and Climatology*, *50*(11), 2270–2282. https://doi.org/10.1175/2011JAMC-D-11-06.1

Zhang, X., Barker, S., Knorr, G., Lohmann, G., Drysdale, R., Sun, Y., et al. (2021). Direct astronomical influence on abrupt climate variability. *Nature Geoscience*, *14*(11), 819–826. https://doi.org/10.1038/s41561-021-00846-6

Zhang, X., Zheng, Z., Huang, K., Yang, X., & Tian, L. (2020). Sensitivity of altitudinal vegetation in southwest China to changes in the Indian summer monsoon during the past 68000 years. *Quaternary Science Reviews*, *239*, 106359. https://doi.org/10.1016/j.quascirev.2020.106359

Zhang, Z., Li, G., Cai, Y., Cheng, X., Sun, Y., Zhao, J., et al. (2022). Millennial-scale monsoon variability modulated by low-latitude insolation during the last glaciation. *Geophysical Research Letters*, *49*(1), e2021GL096773. https://doi.org/10.1029/2021GL096773

Zhao, Y., An, C.-B., Mao, L., Zhao, J., Tang, L., Zhou, A., et al. (2015). Vegetation and climate history in arid western China during MIS2: New insights from pollen and grain-size data of the Balikun Lake, eastern Tien Shan. *Quaternary Science Reviews*, *126*, 112–125. https://doi.org/10.1016/j.quascirev.2015.08.027

Zorzi, C., Sanchez Goñi, M. F., Anupama, K., Prasad, S., Hanquiez, V., Johnson, J., & Giosan, L. (2015). Indian monsoon variations during three contrasting climatic periods: The Holocene, Heinrich Stadial 2 and the last interglacial–glacial transition. *Quaternary Science Reviews*, *125*, 50–60. https://doi.org/10.1016/j.quascirev.2015.06.009

References From the Supporting Information

Anupama, K., Ramesh, B. R., & Bonnefille, R. (2000). Modern pollen rain from the biligirirangan–Melagiri hills of southern eastern Ghats, India. *Review of Palaeobotany and Palynology*, *108*(3–4), 175–196. https://doi.org/10.1016/S0034-6667(99)00039-1

Birks, H. J. B., & Line, J. M. (1992). The use of Rarefaction analysis for estimating palynological richness from Quaternary pollen-Analytical data. *The Holocene*, *2*, 1–10. https://doi.org/10.1177/095968369200200101

Bonnefille, R., Anupama, K., Barboni, D., Pascal, J., Prasad, S., & Sutra, J. P. (1999). Modern pollen spectra from tropical South India and Sri Lanka: Altitudinal distribution. *Journal of Biogeography*, *26*(6), 1255–1280. https://doi.org/10.1046/j.1365-2699.1999.00359

Connor, S. E., van Leeuwen, J. F. N., van der Knaap, W. O., Akindola, R. B., Akindola, R. B., Adeleye, M. A., & Mariani, M. (2021). Pollen and plant diversity relationships in a Mediterranean montane area. *Vegetation History and Archaeobotany*, *30*(5), 583–594. https://doi.org/10.1007/s00334-020-00811-0

Correa-Metrio, A., Bush, M. B., Pérez, L., Schwalb, A., & Cabrera, K. R. (2011). Pollen distribution along climatic and biogeographic gradients in northern Central America. *The Holocene*, *21*(4), 681–692. https://doi.org/10.1177/0959683610391321

Goring, S., Lacourse, T., Pellatt, M. G., & Mathewes, R. W. (2013). Pollen assemblage richness does not reflect regional plant species richness: A cautionary tale. *Journal of Ecology*, *101*(5), 1137–1145. https://doi.org/10.1111/1365-2745.12135

Heaton, T. J., Köhler, P., Butzin, M., Bard, E., Reimer, R. W., Austin, W. E., et al. (2020). Marine20—The marine radiocarbon age calibration curve (0–55, 000 cal BP). *Radiocarbon*, *62*(4), 779–820. https://doi.org/10.1017/RDC.2020.68

Juggins, S. (2020). rioja: Analysis of quaternary science data. R package version 0.9-26. Retrieved from https://cran.r-project.org/package=rioja

Legris, P. (1963). La végétation de l'Inde: Écologie et flore. PhD Thesis. .

Maher, L. J., Heiri, O., & Lotter, A. F. (2012). Assessment of uncertainties associated with Palaeolimnological laboratory methods and Microfossil analysis. In H. J. B. Birks, A. F. Lotter, S. Juggins, & J. P. Smol (Eds.), *Tracking environmental change using lake sediments: Data handling and numerical techniques, developments in paleoenvironmental research* (pp. 143–166). Springer Netherlands. https://doi.org/10.1007/978-94-007-2745-8_6

Nilsson-Kerr, K., Anand, P., Sexton, P. F., Leng, M. J., & Naidu, P. D. (2022). Indian Summer Monsoon variability 140–70 thousand years ago based on multi-proxy records from the Bay of Bengal. *Quaternary Science Reviews*, *279*, 107403. https://doi.org/10.1016/j.quascirev.2022.107403

Pardoe, H. S. (2021). Identifying floristic diversity from the pollen record in open environments; considerations and limitations. *Palaeogeography, Palaeoclimatology, Palaeoecology*, *578*, 110560. https://doi.org/10.1016/j.palaeo.2021.110560

Phillips, S. C., Johnson, J. E., Giosan, L., & Rose, K. (2014). Monsoon-influenced variation in productivity and lithogenic sediment flux since 110 ka in the offshore Mahanadi Basin, northern Bay of Bengal. *Marine and Petroleum Geology*, *58*, 502–525. https://doi.org/10.1016/j.marpetgeo.2014.05.007

Quamar, M. F., & Bera, S. K. (2015). Modern pollen–vegetation relationship in the tropical mixed deciduous forest of the Koriya District in Chhattisgarh, India. *Grana*, *54*(1), 45–52. https://doi.org/10.1080/00173134.2014.946443

Riedel, N., Stebich, M., Anoop, A., Basavaiah, N., Menzel, P., Prasad, S., et al. (2015). Modern pollen vegetation relationships in a dry deciduous monsoon forest: A case study from lonar crater lake, central India. *Quaternary International*, *371*, 268–279. Updated Quaternary Climatic Research in parts of the Third Pole Selected papers from the HOPE-2013 conference. https://doi.org/10.1016/j.quaint.2015.01.046

Thanikaimoni, G. (1987). Mangrove palynology.

Troup, R. S. (1921). The Silviculture of Indian trees. *Nature*, *108*, 3–4. https://doi.org/10.1038/108003a0

Wang, Y. J., Cheng, H., Edwards, R. L., An, Z. S., Wu, J. Y., Shen, C. C., & Dorale, J. A. (2001). A high-resolution absolute-dated late Pleistocene monsoon record from Hulu Cave, China. *Science*, *294*(5550), 2345–2348. https://doi.org/10.1126/science.1064618